
Fracture 1977, Volume 2, ICF4, Waterloo, Canada, June 19 - 24, 1977

ON THE TRANSITION FROM INITIATION TO PROPAGATION OF FATIGUE CRACKS IN PLAIN STEEL SPECIMENS

K. Rahka*

INTRODUCTION

In order to clarify mechanisms of cracking initiation in fatigue observations of the initiation sites of fatigue cracks in plain steel specimens were made with SEM (scanning electron microscope) after final fracture of the specimens. Before fatigue testing specimens were prepared carefully to remove excessive surface roughness and work-hardened layers. Four different steel qualities were used in the testing in seven different treatment modifications.

TEST MATERIALS, SPECIMENS AND EXPERIMENTAL PROCEDURES

The chemical analyses of the steels tested are given in Table 1. Part of the material was fatigue tested in the as received condition and the remainder was subjected to different cold working or heat treatments. These treatments are described in Tables 2 and 3. Examples of the microstructures thus obtained are shown in Figure 1.

Fatigue loading of carefully surface prepared specimens was performed in pulsating tension with mean stress factor $R = \sigma\ \min/\sigma\ \max = 0.05\text{-}0.1$. All fatigue tests were performed in laboratory air with a loading frequency of 50 Hz. Tensile testing was also carried out.

RESULTS

Fatigue and tensile testing results are shown in Figure 2. In Figure 3 scanning electron micrographs of the cracking initiation sites in a few tested specimens are shown. It is seen that the cracking process resulted in different sizes of crack nucleus. The plot of crack nucleus size as a function of tensile stress range in Figure 4 yields a linear relationship as follows:

$$\Delta\sigma = 6200(0.18-a)\mathrm{MPa},(a) = \mathrm{mm} \qquad (1)$$

It can be concluded that this relationship is independent of other factors such as tensile or yield strength and even microstructure. Strictly speaking this is true only for the present testing conditions.

For comparison, a curve derived using, somewhat boldly, a fracture mechanics approach is also shown, e.g.

---

*The Research Council for Technology, the Academy of Finland now with Reactor Materials Research, Technical Research Centre of Finland (VTT). SF-02150-ESPOO 15, Finland.

$$\Delta K = \Delta\sigma\sqrt{\pi a} = 10 \text{ MPa}\sqrt{m} \qquad (2)$$

It is seen in Figure 4 that this curve also fits to the data points fairly well, although systematic deviation can be noted at its both ends.

As can be seen from the SEM micrographs, part of the specimens fractured following crack initiation from inclusions. All inclusion sizes measured from these photographs end up below the curve given above for the relation between a crystalline crack nucleus and the tensile stress range.

DISCUSSION

In this study a linear relationship between the crystalline sliding-tearing mode fatigue crack nucleus and the tensile stress range was obtained. Because several different microstructures were present in the tested materials it can be concluded, that the relation obtained is independent of the microstructure. Strictly speaking, however, the result might be typical of the testing environment, but this fact is outside the scope of this work. The result must be understood at most to be characteristic only of steels with varying microstructural features, because single crystals for instance can behave in a completely different manner (1), having presumably preferred directions for crack growth by fatigue.

The linear relationship above between the tensile stress range and the transition crack size raises questions as to the general applicability of the equation. If a = o then the tensile stress range is $\Delta\sigma$ = 1116.0 MPa. This is very close to the highest fatigue strength value $\Delta\sigma$ = 1120-1210 MPa for ausformed H11 steel [2] reported in the literature. This fact therefore indicates that the achievement of even higher fatigue strength in materials should be possible only by using other strengthening mechanisms than those familiar from commonly used steels. In retrospect the equation (1) would also give a possible maximum size for a, possible in fatigue loading, that is a = 0.18 mm. The truth behind and implications of this fact could be worthy of a study.

An estimate of the stress intensity factor range, at which the fatigue crack would start to grow perpendicularly to the acting tensile stress was estimated above to be about 10 MPa$\sqrt{m}$. This value is close to but somewhat higher than a ΔK_{th}-value (threshold stress intensity factor) reported for steels [3]. Naturally, therefore, it can be concluded that at the ΔK_{th}-value reported in the literature cracking occurs primarily by sliding in plain unnotched specimens.

It should be clear that the critical crack size tolerated possibly indefinitely, the fatigue limit crack size, is smaller than the critical crack size for mode I propagation in plain specimens. This crack size should also be dependent on the metal's microstructure, loading environment and so on.

ACKNOWLEDGEMENT

The author is grateful to Professor Sakari Heiskanan, Head of the Materials and Processing Research Department of the Technical Research Centre of Finland for showing continuous interest in and giving support for the work. Thanks are also due to the Finnish Academy and The Foundation for Technology in Finland (The Rautaruukki Oy Foundation) and the Finnish Cultural Foundation (the Maili Autio Foundation) for continuous financial support during the progress of the work. The materials tested were kindly delivered by OVAKO Oy, Imatra, Finland. This work was done as partof the study for the author's degree of Lic. Tech. at Helsinki University of Technology.

REFERENCES

1. DUQUETTE, D. J., GELL, M. and PITEO, J. W., Met. Trans. 1, 1970, 3107.
2. BORIK, F., JUSTUSSON, W. M. and ZACKAY, V. F., Trans. ASM 56, 1963, 327.
3. POOK, L. P., ASTM STP 513, 1972, 106.

Table 1 Nominal analyses of the steels tested

Steel	C	Si	Mn	P	S	Cr	Ni	Mo	Cu	Sn	Al	Nb
A	.15	.50	1.40	.023	.041	.10	.11	.03	.20	.021		
B	.36	.20	.60	.018	.021	.96	.08	.16	.12	.015		
C	.34	.20	.53	.033	.23	1.54	1.52	.19	.44	.032		
D	.04	.13	.62	.015	.011	3.43	.00	.00	.02	.044	.003	.075

Table 2 Initial and successive bar diameters in the cold drawing procedure. Successive and summed reduction percentages are also given. Note the variants chosen for testing (Roman numerials)

Material		A, B, C			D		
Initial Diameter		I 40 mm			I 42 mm		
			% Reduction Total	Per Pass		% Reduction Total	Per Pass
Drawing Ring Diam.	40				II	9.3	(9.3)
	38	II	9.6	(9.6)	III	18.2	(9.6)
	35	III	23.5	(15.3)	IV	30.6	(15.3)
	32		36.1	(16.3)			
	30		43.6	(12.1)			
	28	IV	51.2	(12.9)			

Table 3 Heat treatment procedures for as received materials

Material	A	B	C	D	Variant
Austenitizing	910 C 15 min	850 C 15 min	850 C 15 min	920 C 15 min	
Cooling	water	oil	oil	water	
Tempering	685 C 1 h	625 C 1 h	650 C 1 h	650 C 1 h	V
	610 C 4min	600 C 1 h	600 C 1 h	635 C 6min	VI
	520 C 1 h	635 C 7min	635 C 7min	550 C 1 h	VII
Cooling after tempering	water				

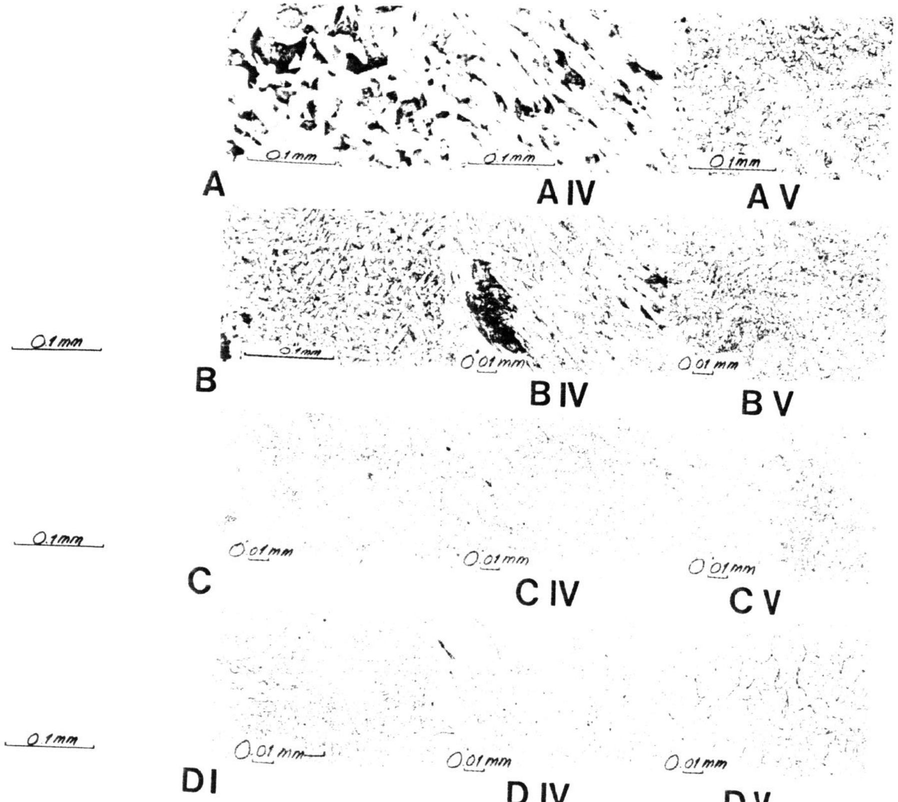

Figure 1 Examples of the microstructures of the tested materials

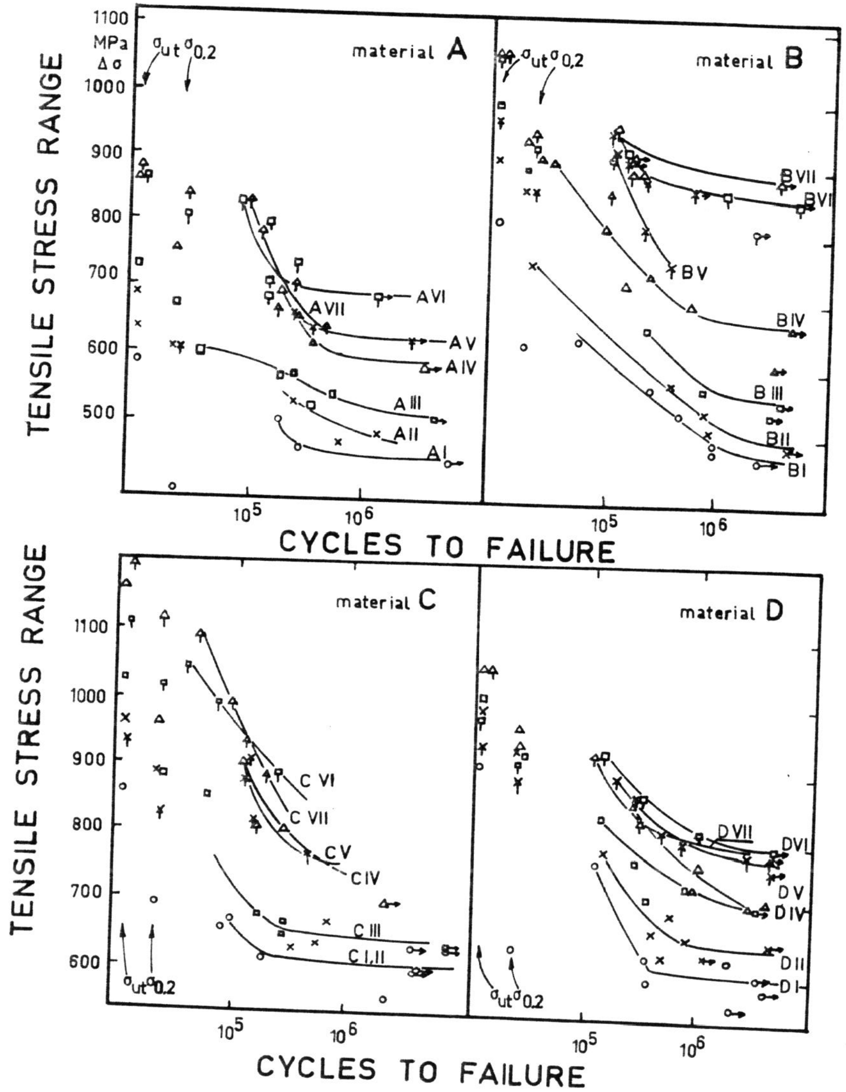

Figure 2 Tensile testing and fatigue testing results for different variants

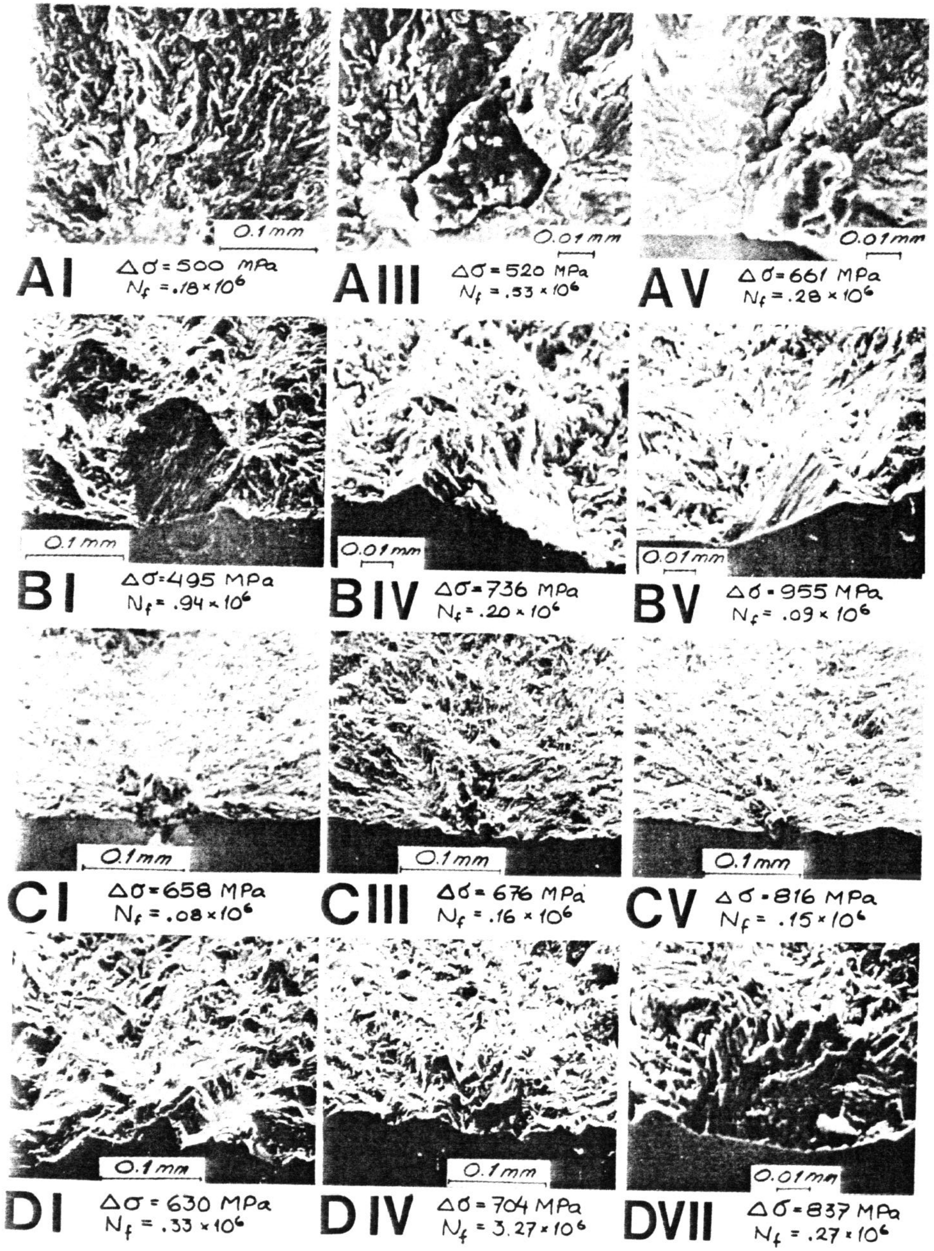

AI $\Delta\sigma = 500$ MPa, $N_f = .18 \times 10^6$

AIII $\Delta\sigma = 520$ MPa, $N_f = .53 \times 10^6$

AV $\Delta\sigma = 661$ MPa, $N_f = .28 \times 10^6$

BI $\Delta\sigma = 495$ MPa, $N_f = .94 \times 10^6$

BIV $\Delta\sigma = 736$ MPa, $N_f = .20 \times 10^6$

BV $\Delta\sigma = 955$ MPa, $N_f = .09 \times 10^6$

CI $\Delta\sigma = 658$ MPa, $N_f = .08 \times 10^6$

CIII $\Delta\sigma = 676$ MPa, $N_f = .16 \times 10^6$

CV $\Delta\sigma = 816$ MPa, $N_f = .15 \times 10^6$

DI $\Delta\sigma = 630$ MPa, $N_f = .33 \times 10^6$

DIV $\Delta\sigma = 704$ MPa, $N_f = 3.27 \times 10^6$

DVII $\Delta\sigma = 837$ MPa, $N_f = .27 \times 10^6$

Figure 3 Cracking initiation sites. N_f=cycles to fracture of test specimen

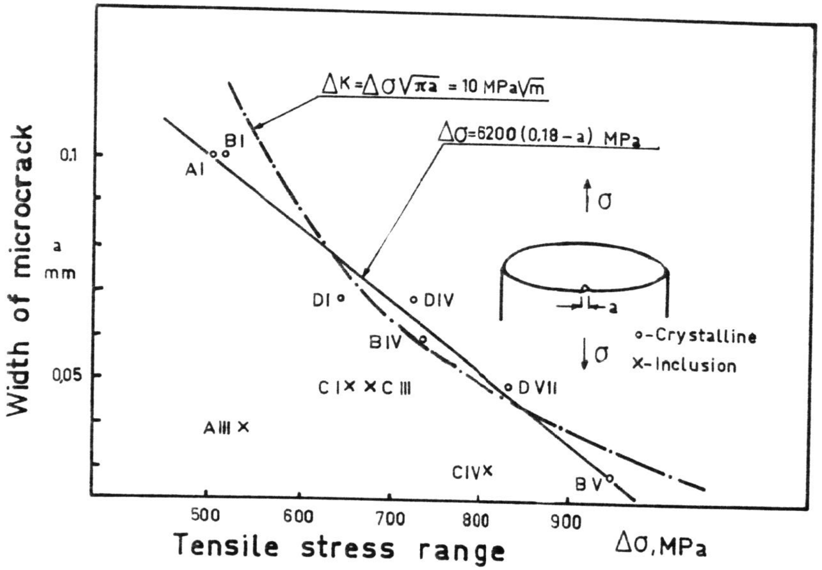

Figure 4 The width of the transition microcrack a as influenced by the tensile stress range